Static model of DH laser

J. Macháč, C.Sc.

Indexing terms: Semiconductor lasers, Modelling

Abstract: A method of complex analysis of the double-heterostructure stripe-geometry laser, based on a new static model, is presented. The optical field distribution in the active region of the laser is described by the wave equation. The interaction between the optical field and free-charge carriers is expressed by the set of rate equations describing also the carrier-concentration profile. Owing to the interaction, it is necessary to solve these equations by a self-consistent procedure. The results of the analysis are light-current characteristics, current dependences of a modal gain, spectra and a near-field pattern. These characteristics are demonstrated in an example.

1 Introduction

The main characteristics describing the behaviour of the laser diode are an optical-field distribution and a free carrier-concentration profile in the active region of the laser. Determination of these functions is the basic step of a laser structure analysis; this knowledge enables us to determine important characteristics of the laser, e.g. light-current characteristics [1, 2], spectra [3] and near- and far-field patterns [4].

The methods of determination and types of laser models have developed in parallel with progress in laser diodes. Attention has been especially directed to the evaluation of field distribution [4, 5]. In the case of stripe-geometry lasers, the main problem is to express and solve the lateral field problem. In lasers with a stripe contact, the optical field is determined by the local gain that is proportional to the carrier concentration. From the other side, the carrier-concentration profile depends on stimulated recombination on the optical field, so that the problem is self-consistent [1, 2, 6] and a proper iterative procedure must be applied. First, carrier-concentration profile is determined from the continuity equation. This profile defines the local gain distribution entering the wave equation. Secondly, the optical problem is solved and a new carrier-concentration profile determined from the modified continuity equation. This procedure is repeated until the threshold condition is satisfied by the proper choice of a mode amplitude.

A new method of finding optical field distribution and carrier-concentration profile is presented in this work. Mode amplitudes cannot be determined directly from the wave equation, because of no suitable source function. These amplitudes are determined separately from the above mentioned work, by the solution of the set of rate equations applied to the steady-state condition of the system. The main advantage of this approach is the possibility of treating a set of longitudinal modes belonging to each oscillating lateral mode and of determining, in this way, together with other laser parameters, a spectrum of the emitted radiation.

The solution is applied to the conventional (Ga, Al)As/GaAs DH laser with a stripe contact and light-current characteristics; current dependence of a modal gain, spectra and a near-field pattern are presented as results of the analysis.

2 Description of analysis

The semiconductor injection laser is a system consisting, from our view, of two parts: the optical field that can be represented by the set of photons in individual modes and the excited semiconductor that can be represented by the set of free-charge carriers injected into the active region. These two subsystems mutually interact. The schematic of the laser structure and the co-ordinate system is illustrated in Fig. 1.

The following simplifying assumptions are necessary for the solution: all functions are assumed to be independent of co-ordinate z and symmetrical about the centre of the active region. The work of the laser is in the fundamental transverse mode, because lasers have thin active layers, also making possible the use of the carrier-concentration profile as a function of one co-ordinate y only. The solution of the wave equation is made for TE modes only, because the light of lasers is almost fully polarised. The current-density distribution in the lateral direction is used according to Reference 7 and is independent of lateral carrier diffusion.

The optical-field distribution $E_y(x, y, z, t) = E'_y(x, y)e^{-j(\beta z - \omega t)}$ is a solution of the wave equation

$$\frac{\partial^2 E'_y(x,y)}{\partial x^2} + \frac{\partial^2 E'(x,y)}{\partial y^2} + [k^2 n^2(x,y) - \beta^2]E'_y(x,y) = 0 \quad (1)$$

where $\beta = \beta_r - j\beta_i$ is the complex propagation constant, ω the angular frequency, $k = 2\pi/\lambda$ the wave number, λ the wavelength and $n(x, y) = n_r(x, y) + jn_i(x, y)$ the refractive index. We have no suitable source function for the evaluation of mode amplitudes, so that the wave equation enables us to determine only the normalised field distribution. In our analysis, this distribution is insufficient. It is suitable to use for the above purpose and for the purpose of description of the interaction between the set of rate equations of both systems. These equations must express the spatial variation of analysed functions [8]:

$$\frac{J(y)}{ed} - \frac{N(y)}{\tau_s} + D\frac{d^2N(y)}{dy^2} - \sum_{i,j} g_{ij}[N(y)]\Phi_{ij}(y) = 0 \quad (2)$$

$$\left[\frac{c}{n_{2r}(\omega_{ij})}G_{ij} - \frac{1}{\tau_{pij}}\right]S_{ij} + \frac{C_{ij}}{\tau_s}\frac{1}{2S}\int_{-S}^{S}N(y)dy = 0 \quad (3)$$

where Φ_{ij} and S_{ij} are the photon flux and the photon density of the ijth mode, respectively; G_{ij} and τ_{pij} are the modal gain and the photon lifetime, respectively; C_{ij} is the spontaneous emission into the ijth modes; $N(y)$ is the carrier-concentration profile; S and d are half the stripe width and the active-layer thickness, respectively; g_{ij} is the local gain; $J(y)$ is the current density and e, D and τ_s the electron charge, the free-carrier diffusion constant and lifetime, respectively; c is the velocity of light in vacuum; i and j are subscripts indicating longitudinal and lateral modes, respectively. Work of the laser is supposed to be on the fundamental transversal mode, so that we need not indicate it by a special subscript. The first rate equation, eqn. 2, is the modified continuity equation. The number of eqns. 3 is equal to the number of excited modes. Both the photon flux Φ_{ij} and the photon

Paper 2371I, first received 15th September and in revised form 30th November 1982

The author is with the Institute of Radio Engineering and Electronics, Czechoslovak Academy of Sciences, Lumumbova 1, 182 51 Prague 8, Czechoslovakia

density S_{ij} are proportional to the second power of the mode amplitude, as described below. Eqns. 2 and 3 thus determine relations between the carrier concentration profile and mode amplitudes.

The set of equations, eqns. 1, 2 and 3, must be solved by an iterative procedure, schematically shown in Fig. 2. The carrier-concentration profile is obtained by solving the continuity equation. This function determines the local gain distribution. Using the profile of the local gain, we perform the solution of the wave equation. Mode amplitudes and the carrier-concentration distribution are determined by the consequent solution of the rate equations, together with the wave equation. The solution is repeated until sufficient conformity between distributions of the optical field determined in two subsequent steps occurs. This conformity is checked by values of mode amplitudes.

3 Solution of equations

The wave equation, eqn. 1, can be solved by dividing the function $E'_y(x,y)$ into two factors:

$$E'_y(x,y) = E_o\psi(x)\phi(y) \tag{4}$$

The solution is performed after Reference 5 and we obtain two equations for the functions $\psi(x)$ and $\phi(y)$. The one for the x-problem is the well known equation describing the field distribution in a sandwiched dielectric waveguide consisting of three layers. The equation for the lateral problem has the form

$$\frac{d^2\phi(y)}{dy^2} + [\nu^2 + j2n_{2r}\Gamma_o k^2 n_{2i}(y)]\,\phi(y) = 0 \tag{5}$$

where ν is a separation constant and Γ_o is the filling factor. The imaginary part of the refractive index can be expressed [9]:

$$n_{2i}(y) = \frac{g(y)}{2k} = \frac{aN(y)-b}{2k} \tag{6}$$

where a, b are functions of the photon energy.

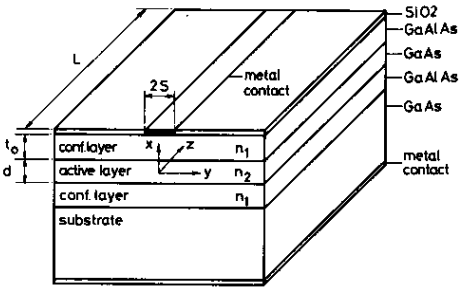

Fig. 1 *Schematic of analysed laser structure*

The function $\phi_j(y)$ for the jth lateral mode is expressed in the form of the set

$$\phi_j(y) = \sum_{v=0}^{v_{max}-1} a_{vj} H'_v(y/S)\, e^{-1/2\,(y/S)^2} \tag{7}$$

We assume that the function $\phi(y)$ does not depend on the wavelength, so that it is the same for all modes with the same lateral subscript j. Similarly, the function $\psi(x)$ does not depend on both subscripts i and j. H'_v are normalised Hermite polynomials of order v. Coefficients a_{vj} are co-ordinates of eigenvectors and separation constants ν^2 are eigenvalues of the characteristic matrix of the wave equation, eqn. 5, obtained using the orthonormal system of the Gauss-Hermite functions $H'_v(y/S)e^{-1/2\,(y/S)^2}$ as a basis. The solution is similar to the method used in the work of Buus [6].

Propagating constants for v_{max} lateral modes are obtained using constants ν_j:

$$\beta_j^2 = k^2 n_{efo}^2 - \nu_j^2 \tag{8}$$

where n_{efo} is the effective refractive index that is evaluated in the solution of the transversal problem.

Mode wavelengths are determined using resonant condition for the real part of the propagating constant β_r:

$$\beta_r(\lambda_{ij}) = \beta_{r,ij} = \frac{i\pi}{L} \qquad j = 0, 1, \ldots, v_{max}-1 \tag{9}$$

where L is the length of the laser and i is an integer representing the number of longitudinal modes. This integer is the longitudinal mode subscript. The function $\beta_r(\lambda)$ can be obtained by solution of the wave equation for several wavelengths, and the resultant dependence is approximated by a continuous function.

The modal gain of the ijth mode G_{ij} is determined by the imaginary part of the propagating constant:

$$G_{ij} = -2\beta_i(\lambda_{ij}) = -2\beta_{i,ij} \tag{10}$$

The photon flux Φ_{ij} is proportional to the power carried by the mode:

$$\Phi_{ij} = \frac{1}{h\omega_{ij}}\,\frac{1}{2}\,\mathrm{Re}(E_{y,ij}H^*_{x,ij}) = Q_{ij}|\phi_j(y)|^2\,|E_{oij}|^2 \tag{11}$$

The photon density S_{ij} is given by energy of the optical field

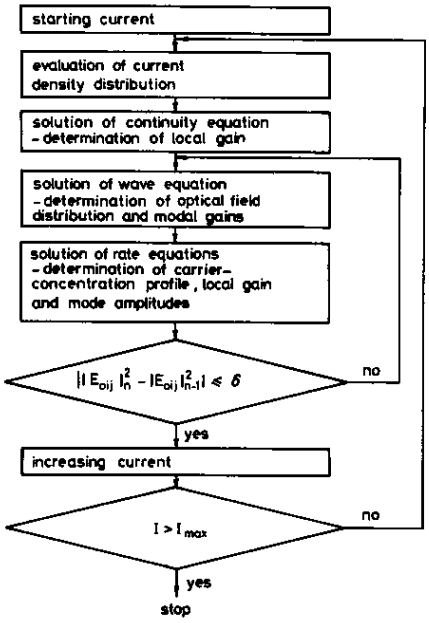

Fig. 2 *Diagram of calculation procedure*

in the laser active region

$$S_{ij} = \frac{1}{\hbar\omega_{ij}V}\frac{1}{4}\epsilon\int_V |E_{ij}|^2\,dV + \frac{1}{4}\mu\int_V |H_{ij}|^2\,dV$$
$$= K_{ij}|E_{oij}|^2 \tag{12}$$

$\hbar$ is the reduced Planck's constant, H the magnetic-field intensity, E_{oij} the mode amplitude, ϵ and μ the permittivity and the permeability of the active region, respectively, $V = 2dLS$ is the active-region volume. The values K_{ij} and Q_{ij} depend on the optical field distribution, the propagating constant and the shape and material constants of the active region. The photon lifetime can be expressed in the form [2]

$$\frac{1}{\tau_{pij}} = \frac{c}{n_{2r}(\lambda_{ij})}\left(\alpha_f + \frac{1}{L}\ln\frac{1}{R_{ij}}\right) \tag{13}$$

where α_f represents optical losses in the active region and R_{ij} is the mirror reflection for the ijth mode.

Eqn. 2 is the modified continuity equation and is solved by a similar method as for the wave equation. Function $N(y)$ has the form of the set

$$N(y) = \sum_{q=0}^{q_{max}-1} \alpha_q H_{2q}(y/S)e^{-(y/S)^2} \tag{14}$$

that simplifies the solution of the wave equation [6]. Eqn. 2 is transformed using set 14, into a system of linear algebraic equations for constants α_q.

Eqns. 2 and 3 are solved by the iterative procedure, together with the wave equation (see Fig. 2). Using the carrier-concentration profile determined in the preceding step, mode amplitudes are evaluated from eqn. 3 in the form

$$|E_{o,ij}|^2 = -\frac{C_{ij}\int_{-S}^{S} N(y)\,dy}{2\tau_e S\left[\dfrac{c}{n_{2r}(\lambda_{ij})}G_{ij} - \dfrac{1}{\tau_{pij}}\right]K_{ij}} \tag{15}$$

These amplitudes are used in the evaluation of a new carrier-concentration profile from eqn. 2, in the following step.

4 Output and input values

The presented mathematical model provides basic characteristics of the laser. The optical field distribution determines the near-field pattern. Mode wavelengths are defined by the resonant condition, eqn. 8. Mode optical power can be calculated from relation [2]

$$P_{ij} = \frac{1}{2}\hbar\omega_{ij}S_{ij}\frac{1}{\tau_{pij}}\mu_{Dij}V \tag{16}$$

where μ_{Dij} is a differential quantum efficiency of the ijth mode. This value can be expressed similarly as in Reference 10:

$$\mu_{Dij} = \begin{cases} \mu_{int}\dfrac{G_{ij}-\alpha_f}{G_{ij}} & \text{for } G_{ij} \geqslant d_f \\ 0 & \text{for } G_{ij} < d_f \end{cases} \tag{17}$$

μ_{int} is an internal quantum efficiency. The total output is a sum of relations 16 over all modes, and its dependence on the pumping current is the light-current characteristic.

The current-density distribution was used according to Reference 7. The dependence of the local gain on photon energy and the carrier concentration has the form of eqn. 6, with a, b being functions of photon energy. Using the approximation of the gain spectra published in Reference 11, we obtain

$$a = 3.24\times10^{-18}(\epsilon - 1.385)^{1.17} \tag{18}$$

$$b = 1.2\times10^{8}(\epsilon - 1.38)^{2.19} \tag{19}$$

where ϵ is the photon energy.

Refractive indexes n_1 and n_{2r} are functions of photon energy; these functions were obtained according to References 12 and 13.

5 Numerical procedure, discussion

The set of equations, eqns. 12, 2 and 3, was solved by the numerical iterative procedure according to Fig. 2. The problem is to evaluate mode amplitudes from relation 15. For currents above threshold, the modal gain is greater than $1/\tau_{pij}$ in the first step of the procedure, and consequently the mode amplitude is negative. This possibility must be eliminated by lowering the modal gain, using the proper choice of mode amplitudes as the first step.

It is necessary to compromise between accuracy and used machine time in the choice of the characteristic matrix order v_{max} and the number of terms in set 14, q_{max}. $v_{max} = 8$ and $q_{max} = 7$ were chosen. The constant δ determining the accuracy of the procedure was chosen for each mode as $\delta = 10^{-4}|E_{oij}|^2$.

The amplitudes of higher lateral modes decrease rapidly with the growth of the order, so that it is enough to confine the solution to the three lateral modes ($j = 0, 1, 2$). It is sufficient to use only 15 longitudinal modes. Thus we have 45 equations 3.

The procedure has been applied to the (GaA1)As/GaAs laser with parameters: length $L = 228\,\mu$m, active-layer thickness $d = 0.25\,\mu$m, internal optical losses $\alpha_f = 5000\,\text{m}^{-1}$, internal quantum efficiency $\mu_{int} = 0.7$, carrier lifetime $\tau_e = 3$ ns, diffusion length $L_{dif} = 3.5\,\mu$m, resistances and thicknesses of the contact and confining layers are $\rho_k = 0.002\,\Omega$m, $\rho_o = 0.01\,\Omega$m, $t_k = 3\,\mu$m and $t_o = 2\,\mu$m.

The light-current characteristics and current dependences of modal gains of the three lowest lateral modes for lasers

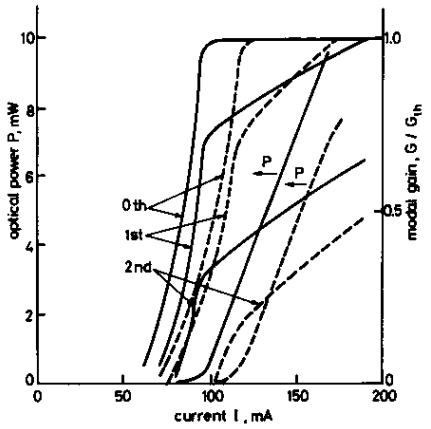

Fig. 3 *Dependence of emitted power and modal gains of first three lateral modes on pumping current*

P = curves for emitted power
——— $S = 6\,\mu$m – – – $S = 9\,\mu$m
$L = 228\,\mu$m, $d = 0.25\,\mu$m, $\alpha_f = 5000\,\text{m}^{-1}$

with contact widths $2S = 12$ and $18\,\mu m$ are shown in Fig. 3. The gain is normalised to the threshold value. The optical power does not include the power of the spontaneous emission. The optical power increases rapidly in the vicinity of the threshold. Owing to the interaction between the optical field and the free-carrier system, the modal gain is saturated; the fundamental mode approaches asymptotically the value $\alpha_f + 1/L(\ln 1/R_{ij})$, whereas the gain of higher modes is only partly saturated.

In the vicinity of the current where the propagation condition of the first lateral modes is satisfied, the procedure described ceases to converge. The solutions of individual steps have an oscillating character. The validity of the model is thus limited to the current interval, up to this point. This critical point is the so-called 'kink' and it defines the critical current I_k and the critical power P_k.

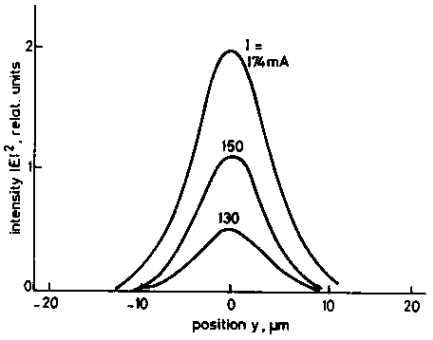

Fig. 4 *Near-field pattern as function of current*
$S = 9\,\mu m$, $L = 228\,\mu m$
$d = 0.25\,\mu m$, $\alpha_f = 5000\,m^{-1}$

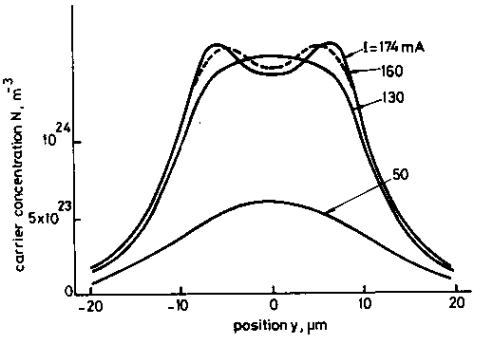

Fig. 5 *Carrier-concentration profile as function of current*
$S = 9\,\mu m$, $L = 228\,\mu m$, $d = 0.25\,\mu m$

The near-field patterns and the carrier-concentration profiles are plotted in Figs. 4 and 5. The dependence of full width at half power (FWHP) of the near-field on the current is shown in Fig. 6. The curves for the stimulated emission start at the threshold of the stimulated emission, where the modal gain equals the optical losses α_f. Below the threshold, the FWHP is determined by the carrier-concentration profile. The near-field is given in the vicinity of the threshold by superposition of the spontaneous and stimulated emissions. An assessed approximation of FWHP in this region (the model does not include spontaneous emission power) is plotted by thinner curves.

The calculated spectrum is in Fig. 7. It can be seen from the detail, that, for currents near I_k, the power of the first lateral modes increases.

The variations of threshold-current density J_{th} and threshold current I_{th} with contact width and optical losses α_f are plotted in Fig. 8. The increase of threshold-current density is the result of the current spreading in the contact and confining layers.

The critical current I_k is greater for the lasers with narrower stripes, as illustrated in Fig. 9, where the critical power P_k is also plotted. If optical losses are increased, the threshold current increases, together with current I_k so that the ratio I_k/I_{th} does not change its value; only the critical power P_k decreases, as illustrated in Fig. 10.

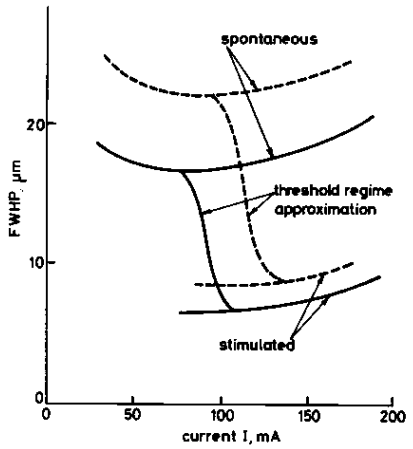

Fig. 6 *Dependence of FWHP of near-field pattern on pumping current*
——— $S = 6\,\mu m$ – – – – $S = 9\,\mu m$
$L = 228\,\mu m$, $d = 0.25\,\mu m$, $\alpha_f = 5000\,m^{-1}$

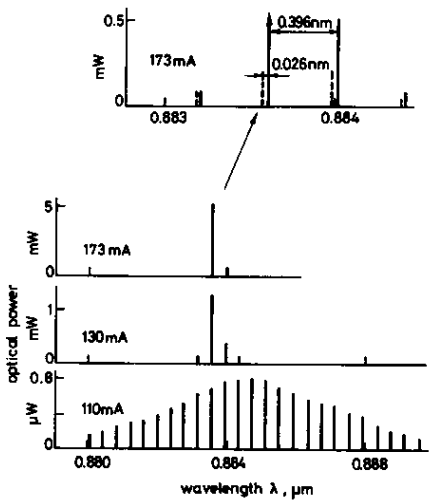

Fig. 7 *Spectra of laser with current as parameter*
In the detail for 173 mA, longitudinal modes belonging to the fundamental lateral mode are plotted by continuous lines and the ones belonging to the first lateral mode are plotted by discontinuous lines
$S = 9\,\mu m$, $L = 228\,\mu m$
$d = 0.25\,\mu m$, $\alpha_f = 5000\,m^{-1}$

The analysis presented does not consider other possible influences on the behaviour of the laser like the effects of temperature and built-in oxide stress etc. The temperature profile across the active region raises the refractive index, and in this way tapers the created waveguide, so that the threshold current decreases [16]. On the other hand, the temperature profile influences the stimulated recombination efficiency and the majority of other laser parameters. Nevertheless, consideration of the temperature effect is very difficult and requires using a selfconsistent procedure.

The results of the analysis can be compared with experimentally obtained data. The dependence of fundamental mode gain, from Fig. 3, is very similar to that obtained by Hakki and Paoli [14]. The spatial hole burning, as in Fig. 5, has been observed, for example, in recent work [17] on InGaAsP/InP lasers. The best way of comparison of near-field patterns is due to FWHP. Fig. 11 illustrates the theoretical dependence of FWHP on normalised pumping current I/I_{th} and measured FWHP. An experiment was made on conventional GaAlAs/GaAs lasers prepared by LPE. Laser parameters are given in the caption of Fig. 11. The Figure shows a good accuracy of the analysis. The calculated spectrum corresponds to the experimentally obtained spectra [3] in the vicinity of the threshold. The spectra above the threshold have a single-mode character that occurs only seldomly in this type of laser (especially lasers with a broader stripe). This fact is probably caused by local gain approximation, eqns. 6, 18 and 19, which does not consider the effects of temperature, spectral hole burning etc. The threshold-current densities given in Fig. 8 correspond with those given, for example, in Reference 18. Similarly, the critical power P_k from Fig. 9 can be qualitatively compared with data given in Reference 19.

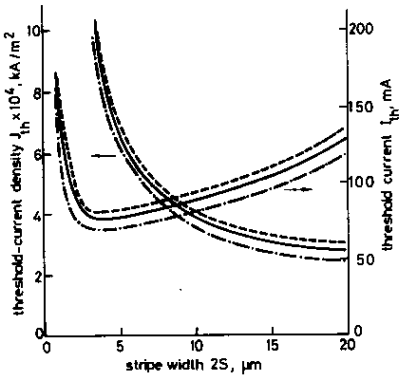

Fig. 8 *Dependence of threshold current density and threshold current on stripe width 2S and optical losses*

– – – – $\alpha_f = 8000\ m^{-1}$ ——— $\alpha_f = 5000\ m^{-1}$ — · — · $\alpha_f = 2000\ m^{-1}$
$L = 228\ \mu m$, $d = 0.25\ \mu m$

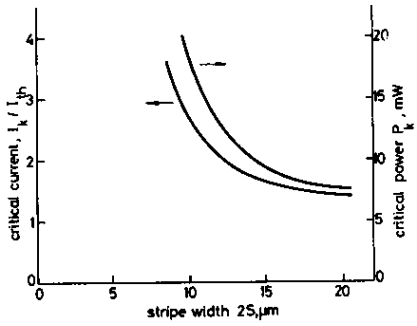

Fig. 9 *Ratio I_k/I_{th} as function of stripe width*

$L = 228\ \mu m$, $d = 0.25\ \mu m$, $\alpha_f = 5000\ m^{-1}$

6 Conclusions

The method of laser diode analysis is described in the paper, providing, as can be seen, a realistic description of the laser. The analysis is based on the solution of the set of rate equations in connection with the wave equation. The rate equations enable us to calculate mode amplitudes determining the emitted power and thus to calculate the spectrum of emitted radiation.

Nearly all laser characteristics are obtained from the calculation. They are light-current characteristics and their parameters: threshold currents, critical currents and powers; near-field patterns, carrier-concentration distributions and spectra. Dependences of the modal gain on the pumping current are determined, together with light-current characteristics. These dependences were for the fundamental lateral mode described, for example, by Biard *et al.* [10] and by Hakki and Paoli [14]. For higher lateral modes, similar dependences have been calculated in recent work [15]. Modal

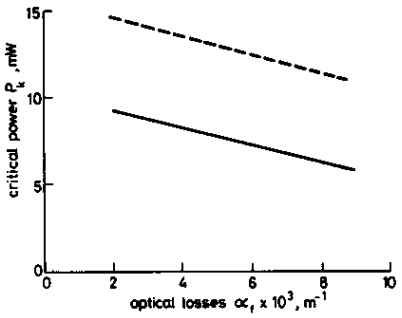

Fig. 10 *Dependence of critical power P_k on optical losses and stripe width*

– – – – $S = 6\ \mu m$ ——— $S = 10\ \mu m$
$L = 228\ \mu m$, $d = 0.25\ \mu m$

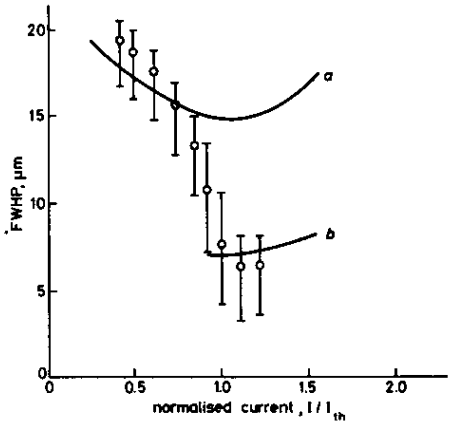

Fig. 11 *Comparison of calculated FWHP and measured data for GaAlAs/GaAs laser*

a Spontaneous *b* Stimulated
$S = 5\ \mu m$, $d = 0.2\ \mu m$, $t_0 = 2\ \mu m$, $\alpha_f = 5000\ m^{-1}$, $t_k = 3\ \mu m$

gains of these modes are saturated only partly above threshold, and kink occurs when the modal gain of the first lateral mode approaches the threshold value. This method enables one, prior to the above-mentioned works [1, 2, 6], to calculate the spectrum of emitted radiation. This has not been done in any published work, but in Reference 3, mode wavelengths have been evaluated.

This method is not confined only to lasers with stripe contact. If the different mechanism of light guiding is expressed in the wave equation, it can be applied to more complicated structures, such as buried-heterostructure lasers or CSP lasers.

7 References

1 LANG, R.: 'Lateral transversal mode instability and its stabilization in stripe geometry injection lasers', *IEEE J. Quantum Electron.*, 1979, QE-15, pp. 718–726

2 CHINONE, N.: 'Nonlinearity in power-output-current characteristics of stripe-geometry lasers', *J. Appl. Phys.*, 1977, 48, pp. 3237–3243

3 NUNES, F.D., PATEL, N.B., MENDOZA, A.J.G., and RIPPER, J.E.: 'Refractive-index profile and resonant modes in GaAs lasers', *ibid.*, 1979, 50, pp. 3852–3857

4 BOTEZ, D.: 'Near- and far- field analytical approximattions for the fundamental mode in symmetric waveguide DH lasers', *RCA Review*, 1978, 39, pp. 577–603

5 STREIFER, W., SCRIFES, D.R., and BURNHAM, R.D.: 'Analysis of gain-induced waveguiding in stripe geometry diode lasers', *IEEE J. Quantum Electron.*, 1978, QE-14, pp. 418–427

6 BUUS, J.: 'Detailed field model for DH stripe lasers', *Opt. & Quantum Electron.*, 1978, 10, pp. 459–474

7 DUMKE, W.P.: 'Current thresholds in stripe-contact injection lasers', *Solid-State Electron.*, 1973, 10, pp. 1279–1281

8 BUUS, J., and DANIELSEN, H.: 'Carrier diffusion and higher order transversal modes in spectral dynamics of the semiconductor laser', *IEEE J.*, 1977, QE-13, pp. 669–674

9 HAKKI, B.W.: 'Carrier and gain spatial profiles in GaAs stripe geometry lasers', *J. Appl. Phys.*, 1973, 44, pp. 5021–5028

10 BIARD, J.R., CARR, W.N., and REED, B.S.: 'Analysis of a GaAs laser', *Trans. AIME*, 1964, 230, pp. 286–290

11 CASEY, H.C., and PANISH, M.B.: 'Heterostructure injection lasers; Part A: Fundamental principles' (Academic Press, New York, 1978)

12 CASEY, H.C., SELL, D.D., and PANISH, M.B.: 'Refractive index of $Al_xGa_{1-x}As$ between 1.2 and 1.8 eV', *Appl. Phys. Lett.*, 1974, 24, pp. 63–65

13 SELL, D.D., CASEY, H.C., and WECHT, K.W.: 'Concentration dependence of the refractive index for *n*- and *p*- type GaAs between 1.2 and 1.8 eV', *J. Appl. Phys.*, 1974, 45, pp. 2650–2657

14 HAKKI, B.W., and PAOLI, T.L.: 'Gain spectra in GaAs double-heterostructure injection lasers', *ibid.*, 1975, 46, pp. 1299–1306

15 WILT, D.P., and YARIV, A.: 'A self-consistent static model of the double-heterostructure laser', *IEEE J. Quantum Electron.*, 1981, QE-17, pp. 1941–1949

16 MATTOS, T.J.S., PATEL, N.B., and NUNES, F.D.: 'Calculation of the threshold current of stripe-geometry double-heterostructure $GaAs-Ga_{1-x}Al_xAs$ lasers, including a self-consistent treatment of the current-temperature dependence', *J. Appl. Phys.*, 1982, 53, pp. 149–155

17 KAWAGUCHI, H., and TAKAHEI, K., 'Direct observation of the spatial hole burning and the saturation of the spontaneous emission in InGaAsP/InP lasers', *IEEE J.*, 1980, QE-16, pp. 706–708

18 TSANG, W.T.: 'The effects of lateral current spreading, carrier out-diffusion, and optical mode losses on the threshold current density of $GaAs-Al_xGa_{1-x}As$ stripe-geometry DH lasers', *J. Appl. Phys.*, 1978, 49, pp. 1031–1044

19 SU, C.B.: 'An analytical solution of kinks and nonlinearities driven by near-field displacement instabilities in stripe geometry diode lasers', *ibid.*, 1981, 52, pp. 2665–2673